Measuring Cooper pair properties in superconducting Nb-Ta foil via Au point-contact spectroscopy

Brandon Toushan[1]

[1]*Department of Physics, Engineering Physics and Astronomy, Queen's University, 64 Bader Lane, Kingston, Ontario, Canada, K7L 3N6*

Using relatively simple point-contact spectroscopy techniques, it is possible to easily demonstrate the quantum phenomenon of Cooper pair condensation within a senior undergraduate-level laboratory. This is performed by first measuring the differential conductance between an electrochemically-etched gold tip and a thin foil of 99% niobium-tantalum alloy, which has been to cooled to a superconducting temperature ($T \lesssim 9K$). The resulting measurements are fit to Blonder-Tinkham-Klapwijk [1] theory using a finite quasiparticle lifetime [2] and the desired electron pair data is found. From our results, we obtain a superconducting gap energy $\Delta \approx 1.9534meV$, a BCS coherence length $\xi \approx 66.4633nm$, and a lower bound to the Fermi velocity $v_F \geq 6.19 * 10^5 m/s$ for 99% niobium-tantalum foil. These results are in good agreement with previous measurements [2][3] done with similar purities however, due to the extremely specific nature of the alloy used, a distinct lack of sufficiently similar results exist, making more comparisons relatively difficult.

I. INTRODUCTION

Superconductivity is a unique physical phenomenon in which specific materials exhibit zero electrical resistance and in special cases expel magnetic flux fields (Meissner effect) under certain conditions, typically extremely low temperatures. Proposed in 1957, Bardeen-Cooper-Schrieffer (BCS) theory [4] describes this phenomenon as a microscopic effect caused by the condensation of electrons into paired boson-like states called Cooper pairs. In extremely simple terms, Cooper pairs are spin-zero bosons created by electrons of opposite spin ($\pm\frac{1}{2}$) binding together [5]. This binding occurs at the transition temperature of a superconductor T_C, when an energy gap/pair-potential energy/binding energy (Δ) opens up. This energy gap forms as a result of it becoming more thermodynamically favorable for electrons to bind together at lower and lower temperatures[2]. Naturally, it follows from this that at absolute zero all electrons will be bound into Cooper pairs due to this thermodynamic property.

In this experiment we seek to demonstrate this phenomenon of Cooper pair condensation via point-contact spectroscopy onto a foil made of 99% Nb-Ta alloy. We are able to accomplish this by applying the same techniques used to measure the differential conductance of a normal metal/normal metal (N/N) junction to a superconducting metal/normal metal junction (N/S) [6]

Similar experiments have been performed for many different metals and alloys along with various iterations of thickness. Such measurements have been performed on all known superconducting materials including various niobium alloys. Due to the extremely specific nature of our chosen alloy (99% Nb-Ta) and material type (foil instead of film) there are many similar experiments but none that are functionally identical. Because of this we are able to compare our results to other experiments that should be quite similar in order to reality-check our results while providing data and further insights for future research to compare too for our specific alloy.

As far as direct applications, superconductors present many novel uses for society at large both today and into the future. Presently, superconductors find usage within within MRI machines and on MAGLEV train technology thanks to their extremely powerful magnetic properties. Looking to the future, superconductors represent the future of multiple fields including energy storage and quantum computing. Thanks to their unique ability to maintain electric currents with zero resistance, superconductors have enormous potential to become the batteries of the future. In addition to this, the quantum mechanical properties possessed by superconductor represent a viable pathway to developing the first quantum computers. This experiment, while not directly related to any particular one of these applications, seeks to help further understand and demonstrate the detailed study of quantum superconductivity at a senior-undergraduate level which has application in all of the aforementioned areas.

II. THEORY AND BACKGROUND

A. N/S Point Contact Transport Regimes

When a lone electron is incident with a N/S junction, a superposition of three different processes occurs simultaneously. These processes are: (1) transmission, (2) reflection, and (3) Andreev reflection, with each having a unique probability of occurring depending on various factors including the energy of the electron, the "height" of the tunneling barrier and the size and resistance of N/S junction itself [2].

The tunneling barrier itself is represented by a dimensionless quantity, Z, which represents the difficulty an electron encounters when crossing the tunneling barrier. A "low" barrier with a value of $Z \approx 0$ allows current to flow uninhibited, while a "high" barrier with a value of $Z \geq 1$ can inhibit cur-

FIG. 1. Differential conductance in the (a) Andreev and (b) tunneling regimes. [2]

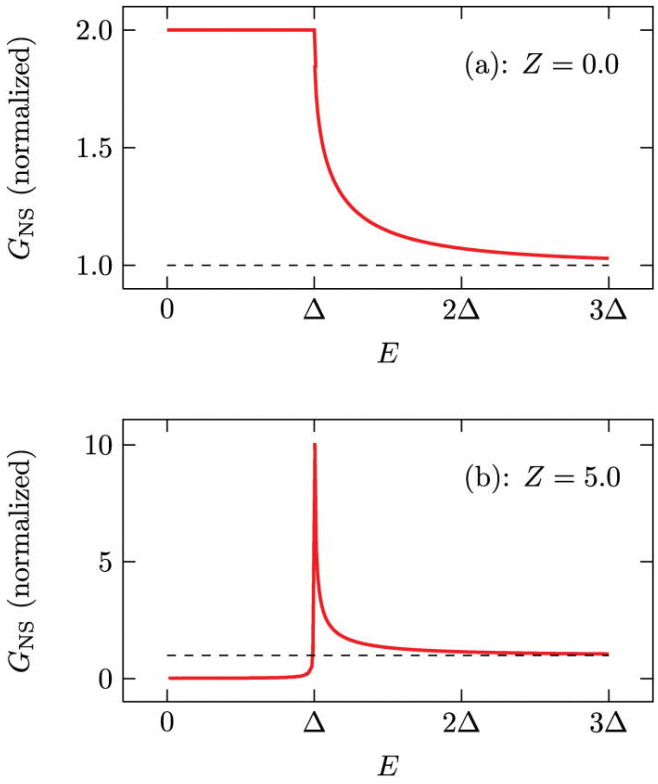

rent drastically [2].

In the first case, when electron pairs have energies above the gap energy Δ, Cooper pairs break apart and form single particle states called "quasiparticles". In this case, process (1), transmission occurs and single electrons are transmitted into the superconductor resulting in constant differential conductance [7]

In the second case, when electron pairs have energies below the gap energy Δ, two outcomes are possible depending on the constriction area. When there is a large constriction area and not enough energy for the incident electron to be transmitted into the superconductor process (2), reflection, occurs resulting in zero differential conductance with a discontinuity at $\Delta = 0$. When there is a small constriction area and enough energy for the incident electron to be transmitted into the superconductor a Cooper pair forms and a "hole" is reflected back and added to the incident current. This case is process (3), Andreev reflection and results in differential conductance increasing by a factor of 2 [7]

B. Solving the BTK Model

As mentioned above, this experiment makes use of the Blonder-Tinkham-Klapwijk or BTK theory to model the Nb-Ta/Au point-contact junction used in this experiment in order

FIG. 2. Andreev reflection diagram [2]

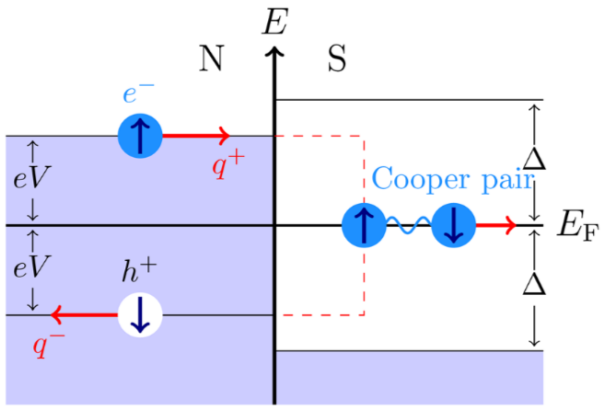

to fit the data and obtain the desired parameters. In simple terms, BTK theory considers the three processes described above (transmission, reflection and Andreev reflection) for a lone electron incident with the boundary of a N/S junction. The potential of the barrier is assumed to be a δ-function barrier with amplitude H, while the energy gap δ is assumed to be constant inside the superconductor [1].

The BTK model is solved using a modified Schrodinger equation known as the Bogoliubov-de Gennes (BdG) equation. The BdG equations extend the Schrodinger equations by accounting for quasiparticle decay Γ, chemical potential μ, and electron-hole coupling (matrices) and are given by [8]:

$$i(\hbar\frac{\partial}{\partial t}+\Gamma\Theta(x))\sigma_z\psi = (\frac{-\hbar^2}{2m}\frac{\partial^2}{\partial x^2}-\mu(x)+V(x))\sigma_z\psi+\Delta(x)\sigma_x\psi \quad (1)$$

Where:
- ψ is the wave-function made up of both the electron wave and the hole wave functions
- σ_x & σ_y are Pauli spin matrices
- Θ is the step function
- $V(x)$ is the potential energy
- $u(x)$ is the chemical potential
- Δ is the energy gap
- Γ is the quasiparticle decay given by:

$$\Gamma = \frac{\hbar}{\tau} \quad (2)$$

When solving the boundary conditions for the continuity of the wave function [2]:

$$\psi_N(0) = \psi_S(0) \quad (3)$$

A discontinuity is found across the δ-function:

$$\frac{-\hbar^2}{2m}(\frac{d\psi_S(0)}{dx} - \frac{d\psi_N(0)}{dx}) + H\psi_S(0) = 0 \quad (4)$$

Following the derivation given in Janson et al., 2012, the probability of Andreev reflection is thus given by [2]:

$$A(E) = aa^* \quad (5)$$

Where:

$$a = \frac{u_0}{v_0}$$

And the probability of normal reflection is given by:

$$B(E) = bb^* \tag{6}$$

Where:

$$b - \frac{(u_0^2 - v_0^2)(Z^2 + iZ)}{\gamma}$$

And:

$$Z = \frac{H}{h v_{Fs}}$$

To find the lower bound on the Fermi velocity of the superconducting material:

$$Z_{eff} = Z^2 = \frac{(1-r)^2}{4r} \tag{7}$$

Where r is the ration of normal/superconductor Fermi velocities:

$$r = \frac{v_{Fn}}{v_{Fs}}$$

C. Fitting Differential Conductance to the BTK Model

Following the derivation detailed in Janson [2], differential conductance at zero temperature is given by:

$$G_{NS} = \frac{dI_{NS}}{dV} \propto N_S(e|V|) \tag{8}$$

Using the BTK formulation to incorporate Andreev reflections [8], the current that flows into the N/S junction is given by:

$$I_{NS} \propto \int_{\infty}^{\infty} (1 + A(E) - B(E))(f(E) - f(E+eV))dE \tag{9}$$

Combining Equations (8) and (9) gives the differential conductance of a N/S junction at low temperature as:

$$G_{NS} = \frac{dI_{NS}}{dV} \propto (1 + A(eV) - B(eV)) \tag{10}$$

By measuring the differential conductance of the N/S junction and fitting it to Equation (10), we are able to obtain values for Z_{eff}, Δ and Γ. [1]

Using Equation (7) and setting $Z = 0$ provides a value for the BCS coherence length [4], given by:

$$\xi = \frac{\hbar v_{Fs}}{\pi \Delta} \tag{11}$$

FIG. 3. Potential energy diagram for the BTK model [2]

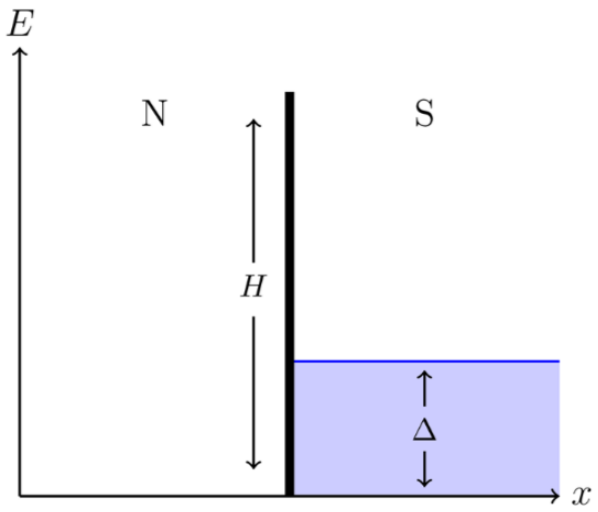

III. EXPERIMENTAL SETUP

A. Apparatus

A Nb-Ta/Au junction is formed by using a differential micrometer to lower an extremely fine gold tip onto the Nb-Ta/Au extremely slowly until a contact resistance of approx 30Ω is measured by a multimeter. The foil used in this experiment was a 0.0127mm thick, 9.93% Niobium, 0.06% Tantalum Nb-Ta. These specifications were not individually verified however and are assumed to have been given as correct from the manufacturer.

The wire contacts to the Nb-Ta sample were soldered into the placed using an indium-lead-tin solder alloy and the specific methods described by A. Leuthold and R. Wakai in their paper, *"Superconducting wire contacts to thin niobium films"* [9]. All wire contacts inside and outside of the dewar were made using this unique solder alloy due to it's unique ability to hold up in extremely low temperature environments such as the one inside the dewar. All solder contacts were then covered with masking tape in order to insulate them and provide as much heat leakage as possible from occurring in order to minimize temperature effects.

The Au tips themselves were electrochemically etched in house just prior to their use in the apparatus. Starting with a 0.5mmm, 99.99% pure gold wire purchased from Alfa Aesar (product #10966), the tips were etched using the methods described by B. Ren et al., in their paper, "*Preparation of gold tips suitable for tip-enhanced Raman spectroscopy and light emission by electrochemical etching*" [24]. A piece of platinum wire was bent into a loop and acted as a cathode, while the gold wire itself acted as the anode. Both anode and cathode were then dipped into 40% HCl solution while an

FIG. 4. The electrochemical etch taking place

offset voltage of 5V was applied. As accurately as possible without automation, most of the Au tips were etched at a depth of $\approx$ $1mm$ with an etch time of 90s. As soon as the etch was completed the tips were gently washed with distilled water to remove any acid and placed within the acrylic holder of the apparatus to minimize exposure to the elements and reduce the risk of blunting and oxidation.

A custom probe arm was built in order to extend the length of a differential micrometer into the inner dewar. This apparatus piece was machined in house according to the specifications used by Janson et al., [2] with some slight differences due to material availability and individual needs. Three brass plates were cut; one to seal the dewar with a soldered inlet tube and an exhaust tube, one to hold the micrometer in place, and one to thread through in order to hold the other two together. The tip holder was also machined custom out of a piece of Teflon along with the plate, the nioibum-tantalum foil was secured to. The dewar itself was made of high-quality hand blown gas and consisted of two parts: an outer dewar filled with liquid nitrogen and an inner dewar filled with liquid helium. The outer dewar pre-cools the system to avoid breakage and insulates the liquid helium while the arm is placed inside the inner dewar to cool the sample to approximately 4.2K, the boiling temp of liquid helium. [10]. All wiring used inside the dewar was Teflon coated in order to ensure durability within the extremely cold environment and the wires themselves were threaded to prevent induced currents and magnetic fields from forming.

The circuity used to obtain the differential conductance measurements was set up to make use of the AC modulation technique in a manner similar to that of Naidyuk et al, in *Point-contact spectroscopy (1989)*" [7] and consisted of an AC voltage source, a variable DC voltage source, a lock-in amplifier, and a multimeter. The AC source produced a 1kHz sinusoidal signal with an amplitude of 280.5mV, while the

FIG. 5. Micrometer arm apparatus

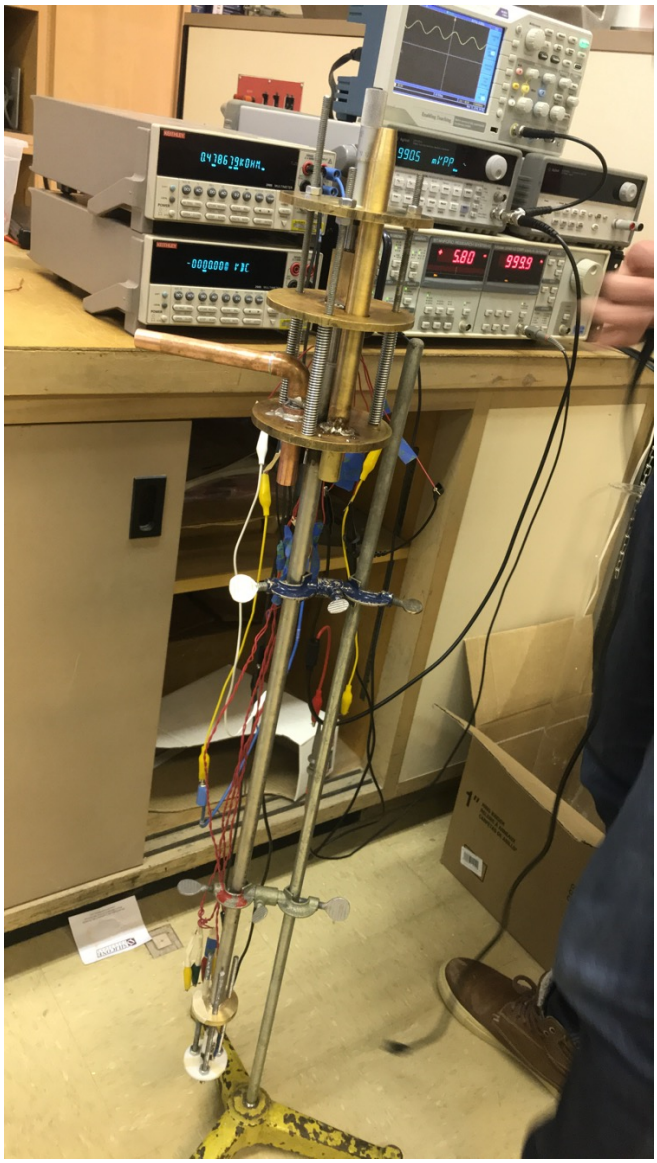

DC source was swept over a range of values from $-3.3V$ to $3.3V$. The Lock-in amplifier was used to isolate the 1kHz signal produced by the AC source from various noise present in the experiment and to measure the output AC voltage across the junction, while the multimeter was used to measure output DC voltage across the junction. Unfortunately, the function generator that was available for the course of the experiment could not sweep through negative values without first flipping the leads. This flip had a dramatic effect on the resistance of our circuit, changing the data itself and forcing us to trim our results after this occurred.

FIG. 6. Circuit Diagram

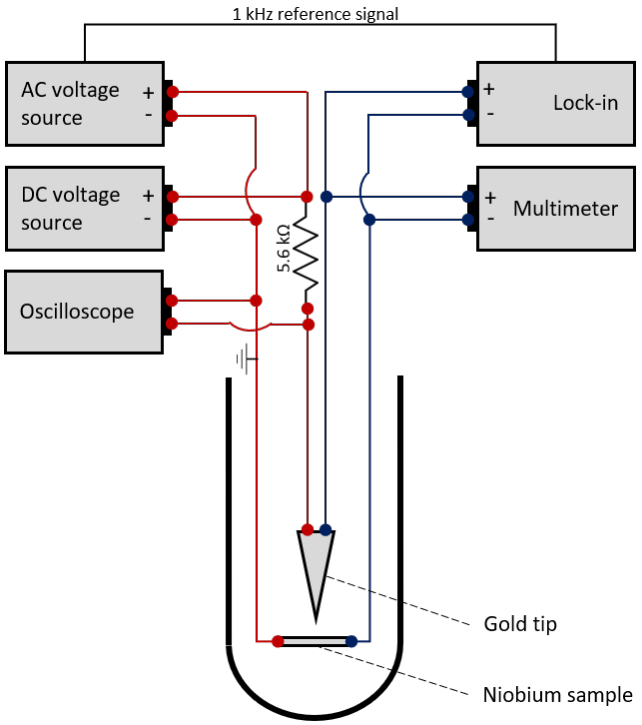

B. Procedure

I) The Nb-Ta sample is cleaned with steel wool & secured in position to the teflon plate at the bottom of the apparatus
II) The Au tip is electrochemically etched just prior to pre-cooling, wired into the circuit and secured in place within the teflon holder
III) The micrometer arm is carefully placed inside the inner dewar while the outer dewar is injected with liquid nitrogen to pre cool. The cooling process then takes approximately two hours to reach adequate temperatures
IV) Once the dewar is cold enough, liquid helium is injected into the inner component and the niobium-tantalum sample reaches superconducting temperatures (<10K) [11]
V) The Au tip is lowered using the micrometer arm until a point contact is made (This occurs when the resistance across the junction measures a resistance between $1\&50\Omega$)
VI) The input AC & DC voltages are then set & a sweep of DC voltages is performed. The resulting DC and AC output voltages are then measured and recorded for each input DC voltage and analyzed

IV. DATA AND RESULTS

As detailed above, the differential conductance was measured using the AC modulation technique described by Naidyuk et al., [7]. The AC voltage measured determines the differential conductance which by Equation (10), is proportional to the probabilities of normal and Andreev reflection. A least squares fit to BTK theory was then performed (see Fig 9) and the desired values were extracted.

Over the course of our experiment 6 trials were performed over 4 superconducting runs. Due to a host of factors, the first 4 trials produced no discernible results and were promptly discarded. These runs failed mostly due to difficulties with the experimental apparatus and our own understanding of the circuitry. Trial 5 was far more in line with expectations and our first successful run. Although the data was still not ideal due a drastic shift in resistance that occurred during the run due to what we believe were heating effects from taking too long to record enough data. Improvements were made again and Trial 6 was performed using the exact setup as Trial 5 just with better execution across the board.

Trial 6 resulted in a wide curve, consistent with expectations in literature. Overall a great success in terms of data-taking, we did still experience a sharp change in resistance near the end of the run due to having to alter our circuitry in order to sweep through negative values. As these incorrect values were caused by instrumental error they were removed from the data for analysis. It was found that the differential conductance we measured fits extremely well to theory upon fitting to BTK theory via a least squares fit. The contact resistance for this trial was measured to be roughly 30Ω, which while higher than expected can be explained by the fact that we used a far thicker foil than the standard evaporated films used in other experiments we compared our data with. The recorded AC and DC voltages were shifted to account for the DC offset ($-1.88mV$) converted to normalized differential conductance and can be seen below, along with the fit to BTK theory (Figs. 7,8 & 9)

TABLE I. Results at 30Ω (Trial 6)

Variable	Value	Uncertainty
$\Gamma(meV)$	0.76919177692	0.019019434891
Z_{eff}	0.418876030391	0.00454411681514
$\Delta(meV)$	1.95344288891	0.0264678800185

TABLE II. Comparison of Estimated Values to Literature

Variable	Trial 6	Janson et al.,	Park et al.,
$v_{Fs}(m/s)$	$6.19 * 10^5$	$3.1 * 10^5$	$5.8 * 10^5$
ξ(nm)	66	43	97
$\Delta(meV)$	1.95	1.53	1.25
Z_{eff}	0.42	0.82	0.453
$\Gamma(meV)$	0.77	0.78	0.55

Upon observing the results in the tables above, it is clear that our results are in good agreement with prior experiments done by both Park et al., [3] and Janson et al., [2]. our Δ and Γ were found to be in better agreement with the results recorded by Janson et al., while our Fermi velocity bound and coher-

FIG. 7. AC voltage vs DC voltage (Trial 6)

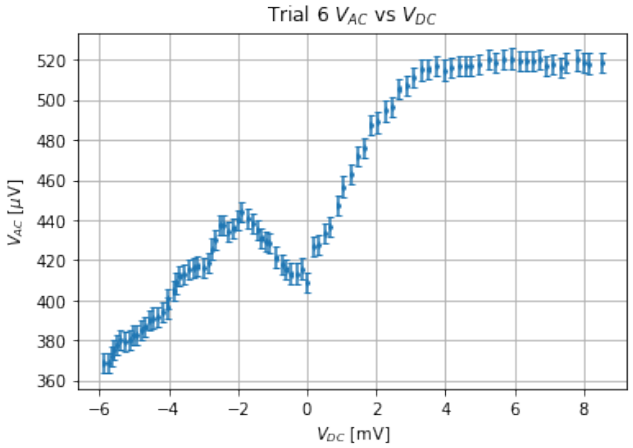

FIG. 8. Normalized differential conductance (Trial 6)

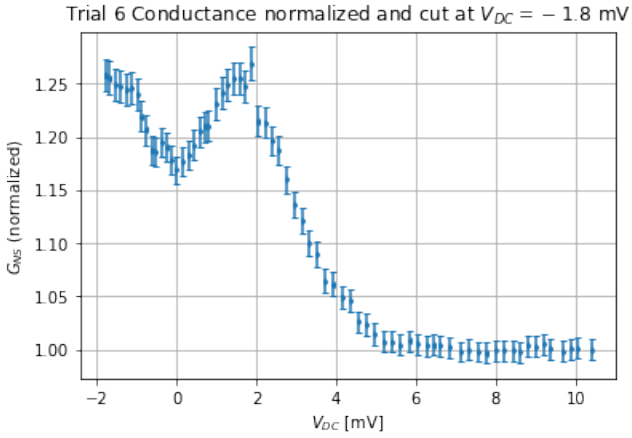

ence length were found to be in better agreement with Park et al's., results. These differences can be explained by the fact that while we used a Nb-Ta alloy both Janson and Park used pure niobium, however the Park experiment was able to better guarantee it's purity. Both Janson and Park used evaporated films while our sample was merely a thin metal foil. Due to the very intricate nature of the phenomenon it is quite difficult to make accurate predictions as to why our data is similar to other sets and not to others however we do have have some guesses as to why. It is our belief that our Δ and Γ values were closer to the Janson et al., values because the niobium they used was less pure than that used by Park and thus closer to ours. Also, we feel that the potential cause of both us and Park et al., recording a greater coherence length and lower fermi velocity bound is due to the ion milling procedure underwent by Janson et al. This process removed moisture out of the metal on a microscopic scale, something not done by either Park et al, or us. This extra moisture relative to Janson et al's., data may have caused an increase in coherence length leading to Park et al, and this experiment measuring larger coherence lengths for similar metals.

V. DISCUSSION

Naturally, the results of this experiment differ somewhat from other similar niobium/gold experiments such as those performed by Janson et al., and Park et al.,. It is a natural question to ask why our differential conductance (Fig 9.) at 30Ω contact resistance shares shares the same shape as a 3Ω in Janson et al., [2] or why some of our values agree better with Janson while others agree better with Park. Without repeating what was already mentioned above, the simple answer to this question is that due to the extremely delicate and specific nature of these experiments exact comparisons cannot me made between any of the three experiments. Despite all the similarities between the Janson and Park

FIG. 9. Normalized differential conductance fit to BTK theory (Trial 6)

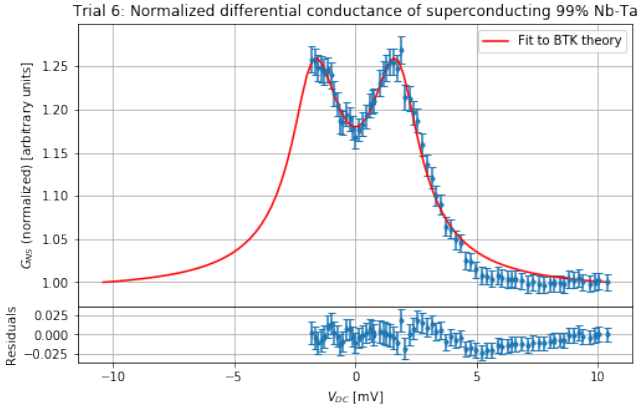

papers, massive differences arise due to both the materials available and the exact metal used. Merely introducing slight impurities into a superconducting material can radically changes it's properties so much so that even it's critical temperature can change drastically. Contact resistances between a point-contact are so extremely delicate that any interference or volatility present in the environment around the system or within the system itself can have a profound impact results. Simply put, at the subatomic level innumerable differences arise relative to even the slightest difference in experimental apparatus and technique such that, something as minor as ion-milling your superconductor prior to use to remove moisture can have a profound impact on results.

Overall, the uncertainty of this experiment was kept quite low. This was made possible due to the sophisticated nature of the circuitry components used and the amount of man-hours that went into operating them correctly. Sources of systematic error outside of potentially malfunctioning circuity are few and far between, and the good agreement between

our results and values in literature shows that this eventuality is highly unlikely. Despite this lack of systematic error, sources of experimental error abound and may include variations of contact pressure due to the volatility of the liquid He environment, temperature effects as a result of the heat pollution inside the dewar increasing during the experiment, possible oxidation effects on both the Au tip and Nb-Ta foil as well as too few trials to fully verify results. Most of these issues can be easily remedied in the future with more and more trials although the cost per trial is quite prohibitive due to the need for large amounts of liquid helium and gold wire per run.

In the future, given unlimited time and resources we have several plans to improve the experiment in terms of both ease of use and experimental accuracy and precision. First, when building the apparatus again we would use the thinnest steel tubes and brass plates available in order to reduce the thermal conductance of the system as much as possible to minimize heat effects. Next, a calibrated thermocouple would be added and calibrated in order to verify that the foil itself is indeed reaching superconducting temperatures and to measure what these critical temperatures are. Next, we would have to gain access to some form of portable fume hood in order to allow us to etch the Au tips in place within the Teflon holder. This would make the entire tip change process drastically easier while reducing the risk of the tip oxidizing or blunting and improve our point-contact. This etch would be completed right next to the dewar itself and the apparatus would then be immediately inserted and eliminating many environmental risks. Naturally, we would also love to have access to a more sophisticated function generator that can sweep positive to negative without having to flip leads and alter the circuitry. This would allow us to complete our data sweep without trimming and enrich our results while improving our ability to fir the data to theory. Last, given time and resources to do many more trials we would like to complete this experiment with both the thin,evaporated film used by Janson et al., and Park et al. Doing this would allow us to use the exact same apparatus and technique on the two different contact styles and enable us the ability to compare them to one another far more accurately.

VI. CONCLUSIONS

The quantum phenomenon of Cooper pair condensation can be readily demonstrated within a senior-undergraduate level laboratory using the same point-contact spectroscopy techniques used for various other differential conductance experiments.During the course of the experiment, it was observed that the values for the energy gap, coherence length and the measured Fermi velocity bounds were within good agreement with prior recorded results in literature. Experimental uncertainty was kept quite low throughout due to the nature of the experiment however, differences between our data and literature values did arise due to the purity of the Nb-Ta foil, dulling and oxidation of the gold tip, and potentially temperature effects occurring inside the dewar apparatus. In the future these problems would be remedied by testing multiple foils and films of different purities, etching the gold tip in place and using more sophisticated data-taking programs to record more data, faster. Overall the managed to demonstrate the Cooper pair condensation effect quite clearly and with slight tinkering and simplification, could easily be reduced down to fit into a senior undergraduate-level lab course on a smaller time-scale.

ACKNOWLEDGMENTS

Team SuperCOOP (Brandon Toushan, James Barron, Tristan Menard and Thomas Mosher) would like to extend special thanks to: Bernie Ziomkiewicz, Steve Gillen, Dr. Marsha Singh, Dr. Marc Dignam, Charles Hearns, Patrick Given & Ananthan Karunakaran for all their time, help and hard work making this experiment possible

[1] G. E. Blonder, M. Tinkham, and T. M. Klapwijk, Phys. Rev. B **25**, 4515 (1982), URL https://link.aps.org/doi/10.1103/PhysRevB.25.4515.

[2] L. Janson, M. Klein, H. Lewis, A. Lucas, A. Marantan, and K. Luna, American Journal of Physics **80**, 133 (2012), https://doi.org/10.1119/1.3660665, URL https://doi.org/10.1119/1.3660665.

[3] W. K. Park and L. H. Greene, Review of Scientific Instruments **77**, 023905 (2006), https://doi.org/10.1063/1.2168670, URL https://doi.org/10.1063/1.2168670.

[4] J. Bardeen, L. N. Cooper, and J. R. Schrieffer, Phys. Rev. **108**, 1175 (1957), URL https://link.aps.org/doi/10.1103/PhysRev.108.1175.

[5] Nobelprize.org, *The nobel prize in physics 1972* (2014), URL https://www.nobelprize.org/nobel_prizes/physics/laureates/1972/.

[6] Y. G. Naidyuk and K. Gloos, *Anatomy of point-contact andreev relfection spectroscopy from the experimental point of view (review)* (2008), URL https://arxiv.org/ftp/arxiv/papers/1712/1712.06903.pdf.

[7] Y. G. Naidyuk and I. K. Yanson, arXiv:physics/0312016 (2003), URL https://arxiv.org/pdf/physics/0312016.pdf.

[8] A. Lucas, problem Collection, URL https://web.stanford.edu/~ajlucas/The%20BTK%20Model.pdf.

[9] A. Leuthold and R. Wakai, Cryogenics **35**, 149?150 (1995).

[10] M. O. Kimball, *Introduction to liquid helium* (2014), URL https://cryo.gsfc.nasa.gov/introduction/liquid_helium.html.

[11] A. Ikushima and T. Mizusaki, Journal of Physics and Chemistry of Solids **30**, 873 (1969), ISSN 0022-3697, URL http://www.sciencedirect.com/science/article/pii/

0022369769902832.

[12] T. Kent, *Experimental low temperature physics* (Springer Science & Business Media, 1993).

[13] C. Kittel, *Introduction to Solid State Physics* (Wiley, 2005), ISBN 9780471415268.

[14] N. W. Ashcroft and N. D. Mermin, *Solid State Physics* (Harcourt College Publishers, 1976), ISBN 0030839939.

[15] J. W. Ekin, *Experimental Techniques for Low-Temperature Measurements: Cryostat Design, Material Properties, and Superconductor Critical-Current Testing* (Oxford University Press, 2006), ISBN 9780191524691.

[16] Nobelprize.org, *The nobel prize in physics 1913* (2014), URL https://www.nobelprize.org/nobel_prizes/physics/laureates/1913/.

[17] J. Eck, *The history of superconductors* (2017), URL http://www.superconductors.org/History.htm.

[18] E. L. Wolf, *Principles of Electron Tunneling Spectroscopy*, vol. 152 (Oxford University Press, 2012), second edition ed.

[19] W. McMillan and J. Rowell, Tech. Rep., Bell Telephone Labs. Inc., Murray Hill, NJ (1969).

[20] B. Hobbs, *Superconductors are so cool right now...* (2011), URL http://www.abc.net.au/science/articles/2011/07/20/3273635.htm.

[21] B. Ren, G. Picardi, and B. Pettinger, Review of Scientific Instruments **75**, 837?841 (2004).